Small and Large Signal Modulation of 850 nm Oxide-Confined Vertical Cavity Surface Emitting Lasers

K. L. Lear, V. M. Hietala, H. Q. Hou, M. Ochiai,
J. J. Banas, B. E. Hammons, J. C. Zolper, and S. P. Kilcoyne

Sandia National Laboratories, PO Box 5800 / MS 0603, Albuquerque, NM 87185-0603

Abstract

The high speed performance of GaAs quantum well, oxide-confined, vertical cavity surface emitting laser diodes is presented. Ion implantation reduces device capacitance resulting in small signal modulation bandwidths up to 21.5 GHz. Analysis and temperature dependent data show the lasers are thermally rather than intrinsically limited. Large signal data rates up to 12 Gb/s are presented including pattern dependent jitter resulting form variable turn-on delay.

Key Words

VCSEL; High speed laser diodes; Microwave frequency response

Introduction

VCSELs are attractive sources for high data rate, economical, fiber communications in local area networks and other applications with rapidly growing bandwidth requirements. We have previously demonstrated record modulation bandwidths for oxide-confined vertical cavity surface emitting lasers (VCSELs) based on strained InGaAs/GaAs quantum wells[1]. The monolithic oxide-confined structure[2] provides good optical confinement, low thresholds, efficient operation, and acceptable thermal resistance; these qualities promote high speed operation. Here we report work on nominally 850 nm wavelength oxide-confined VCSELs with modulation bandwidths in excess of 20 GHz. This shorter wavelength is more attractive because of its greater compatibility with data communications standards. Large signal modulation appropriate to such systems is also discussed below. In particular, the limitations imposed by turn on delay for various bias conditions are quantified for this type of VCSEL structure.

Laser Structure

High modulation bandwidths were achieved with an oxide confined VCSEL structure modified to decrease parasitic circuit elements. The devices reported here utilized an inverted doping approach detailed previously[3] with the n-mirror above the active region to reduce resistance and promote single mode operation by reducing current crowding. Figure 1 shows a schematic cross section of the VCSEL with a corresponding small signal equivalent circuit. Coplanar waveguide pads designed for on wafer probing were placed on a 5 μm thick polyimide to reduce the capacitance between the pad and the conducting

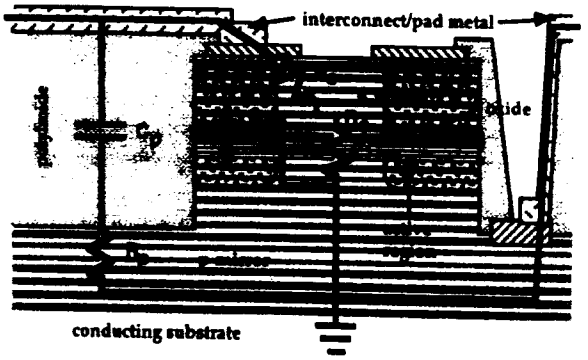

Figure 1. Schematic cross section of high speed VCSEL structure with superposed equivalent circuit.

OSA TOPS Vol. 15 Advances in Vertical Cavity Surface Emitting Lasers, Connie Chang-Hasnain (ed.)

substrate to approximately 50 fF. The device capacitance was further reduced by implanting the mesa area lying outside the active region where thin oxide layers would otherwise result in high capacitance. The electrical effects of the implant were evaluated by looking at the changes in the laser's microwave vector impedance. The magnitude and phase of the associated reflection coefficient are plotted in Figure 2. Device capacitance is evident in the phase change with frequency. Higher levels of implantation decrease the phase change associated with the capacitance.

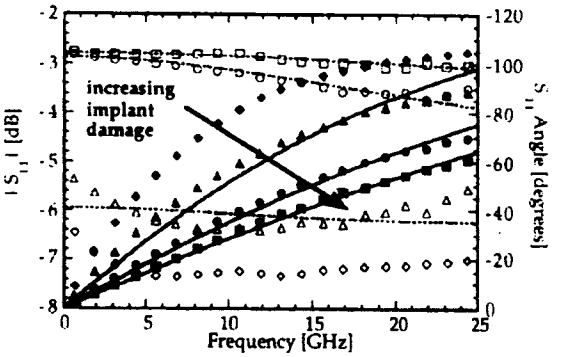

Figure 2. The magnitude (open symbols) and phase (closed symbols) of a small VCSEL's impedance at microwave frequencies. Lines show equivalent circuit fits.

This is quantified by adjusting the parameters of the equivalent circuit in Figure 1 to obtain a fit to the data of Figure 2. The resulting parameters are presented in Table 1 showing that the capacitance is clearly reduced by implantation. The implants also increase the resistances, but the net effect is an increase in electrical bandwidth. At low levels of implant, the maximum observed laser bandwidth is comparable to the electrical bandwidth. At higher levels the observed bandwidth becomes larger than the calculated bandwidth indicating the laser is no longer principally limited by electrical circuit effects.

Table 1. Equivalent circuit parameters for different levels of implants and corresponding calculated electrical bandwidth.

Implant Level	R_s [Ω]	R_a [Ω]	C_a [fF]	$f_{-3dB,elec}$ [GHz]
low	31.3	120.4	152.1	18.8
medium	36.3	269.6	72.9	25.8
high	28.3	288.7	44.3	36.4

Data taken at 2V bias. The pad capacitance and associated resistance were taken as C_{pad}=41.65 fF and R_{pad}=15.9 Ω based on measurements of an isolated pad.

The implant may also enhance the high speed performance by providing recombination centers that reduce the charge storage in the area just outside the oxide aperture. The reduced carrier levels also increase perimeter optical loss encouraging extended single mode operation.

The laser diodes feature DC characteristics that are important for high speed modulation as well. Figure 3 shows quasi-static light-current and voltage-current characteristics indicating a submilliampere threshold current, operation to several times threshold before thermal rollover, good efficiency coupled into the fiber, and moderate resistance for this size of device (~4x4 μm^2). This device operated in the fundamental mode to approximately 4 mA as necessary to obtain increasing photon densities in the mode. Other similar sized devices remained single-mode at all operating currents.

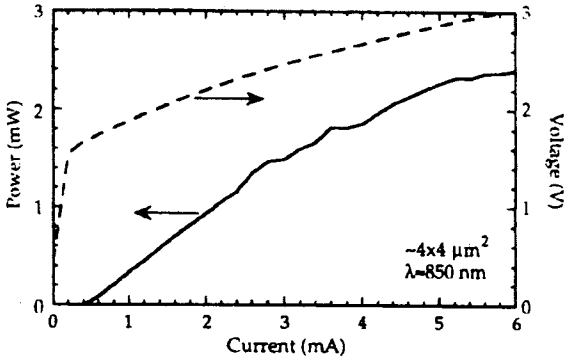

Figure 3. Fiber coupled power and voltage vs. current for a high speed single mode VCSEL.

Small Signal Modulation

The small signal response of VCSELs as a function of bias current was measured using a calibrated vector network analyzer with on wafer probing and a 30 GHz photodetector connected through approximately 2 m of the multimode fiber. The modulation response of a ~4x4 μm^2 single mode laser with a 0.5 mA threshold current is shown in Figure 4 for various bias currents. This optical link reached a maximum bandwidth (3 dB down from the low frequency response) of 21.5 GHz at a bias current approximately ten times threshold. Typical maximum bandwidths were 19 GHz or higher. The droop in response at low (< 5 GHz) frequencies may be partially attributed to the detector performance. A 1.5 dB decrease was measured for the detector at a

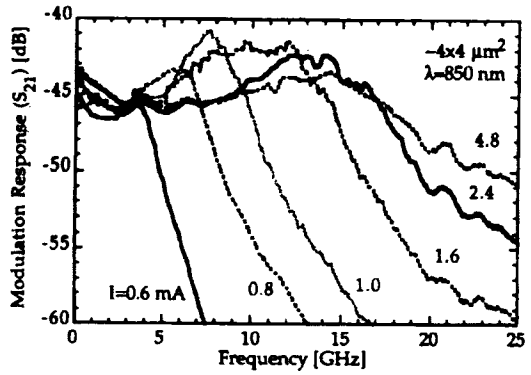

Figure 4. The modulation response of a single mode VCSEL for varying bias currents.

1300 nm wavelength using a lightwave analyzer. This detector response has not been factored out of the data.

The data of Figure 4 was fit with a traditional damped resonator model to extract the resonant frequency and equivalent damping frequency ($\gamma/2\pi$) as shown in Figure 5. A $f^{0.1}$ factor was included to account for the low frequency droop and thus improve the fit. At low bias currents, the bandwidth and resonant frequency increase in proportion to the square root of the current above threshold as expected from the conventional rate equation analysis. The rate of increase in this region yields a modulation current efficiency factor (MCEF) of 14.2 GHz/√mA which is slightly lower than the highest value we previously reported for oxide confined VCSELs with InGaAs quantum wells[1]. Other workers have also obtained an 14 GHz/√mA

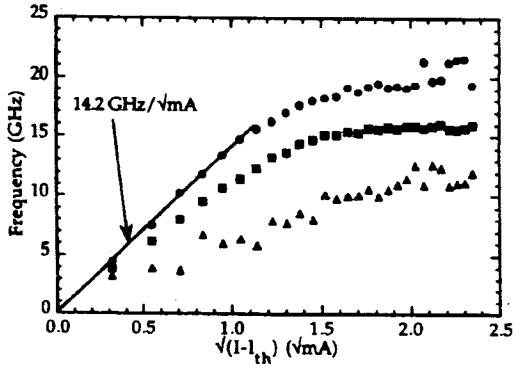

Figure 5. Resonance frequency (squares), -3dB frequency (circles), and equivalent damping frequency($\gamma/2\pi$) (triangles) as a function of square root of current above threshold.

MCEF and a maximum 15.1 GHz bandwidth from an InGaAs VCSEL biased at 2.1 mA[4]. Here the bandwidth increases steadily to 15.5 GHz at 1.7 mA and then begins to saturate. Based on the damping factor's parabolic dependence on the resonant frequency, the intrinsic limits of the laser diode can be extrapolated from the data prior to saturation. This analysis yields a factor of K=0.159 ns which in conjunction with an zero current intercept of the damping constant γ_0=18.8/ns predicts an intrinsic bandwidth limit of 58 GHz. The deviation from linearity in the light vs. current curve in Figure 3 above 4 mA can be attributed to thermal effects and further suggests that the saturation in bandwidth in a similar regime may be associated with decreased differential gain due to self-heating.

This conclusion is further supported by temperature dependent measurements. A nominally identical laser to that discussed above was characterized in wafer form on a variable temperature chuck. The bandwidth as a function of current extracted from this data is plotted in Figure 6 for varying temperatures. At 25 C, the bandwidth is similar to that for the preceding room temperature measurements. A higher ambient temperature shifts the internal temperature upward so that bandwidth saturation occurs with less self-heating and thus at lower currents where the bandwidth is reduced. Nevertheless, the laser still operates to 15 GHz at 100 C and corresponds to the bandwidth performance of the laser at 25C at lower currents. At both 25 and 100 C, the laser reaches 10 GHz with a bias current of approximately 1.1 mA. Lower stage temperatures extended the current range prior to self-heating

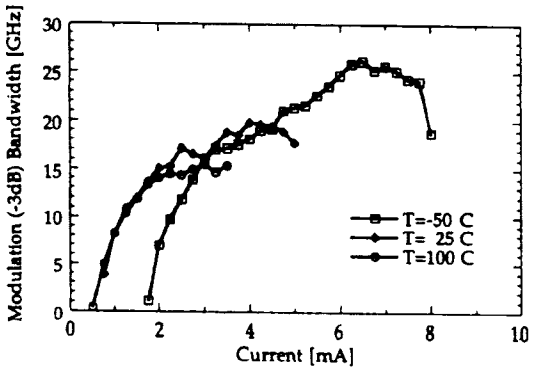

Figure 6. VCSEL bandwidth vs. current bias at three temperatures.

induced bandwidth saturation so that at -50C the laser attains a bandwidth of 26 GHz. At this temperature increased threshold current is necessary to heat the device sufficiently to shift the gain and cavity mode back into alignment. Reduced self-heating through more efficient operation and reduced thermal resistance should extend the bandwidth of oxide-confined VCSELs.

Large Signal Modulation

Large signal, digital modulation experiments were also performed using a 12Gb/s bit error rate tester and 26 GHz sampling oscilloscope. Figures 7 and 8 respectively show the dc light and voltage vs. current and frequency response for larger ~8x8 μm^2 multimode lasers which were initially investigated for large signal modulation. The link used the same photodetector as before with the addition of a ~9 dB, 18 GHz inverting amplifier. Eye diagrams and bit error rates were obtained

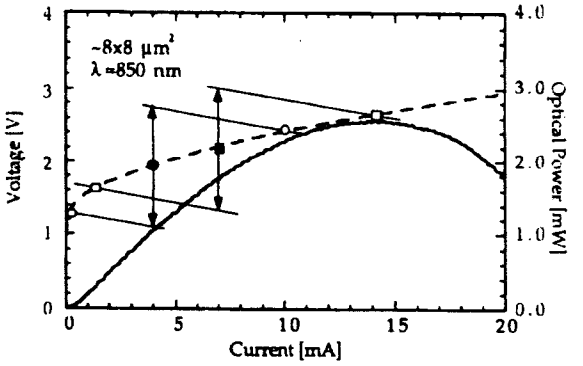

Figure 7. The light and voltage vs. Current characteristics for a multimode VCSEL. Bias and modulation conditions are indicated as discussed in the text.

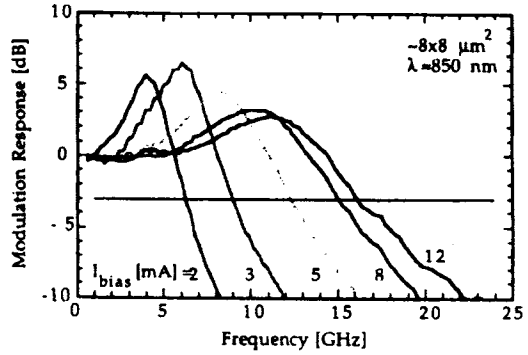

Figure 8. The modulation response of a multimode VCSEL for varying bias currents.

using a 2^7-1 pseudorandom bit sequence (PRBS). The short word length was necessitated by the 45 MHz low frequency cutoff of the amplifier. When the multimode laser was biased at 7 mA and modulated with emitter coupled logic (ECL) voltages as indicated by the squares in Figure 7, an open eye diagram was obtained up to 12 Gb/s as shown in Figure 9. Keeping in mind the signal level inversion caused by the amplifier, the pattern shows overshoot and ringing due to the multimode laser's relaxation resonance which is also apparent in the modulation response shown in Figure 8. Later experiments on the smaller single mode lasers showed much less overshoot due to the ability to drive those devices closer to a critically damped condition. The overshoot could of course be reduced by an appropriate electrical filter that limited the bandwidth further. Even without the filter, bit error rates as low as 10^{-13} were observed in preliminary investigations at 12 Gb/s.

Improved contrast ratios and simplified driving circuits motivate operating the laser so that the low drive level is below threshold if possible. Biasing the multimode laser at 4 mA, indicated by the circles in Figure 7, results in this mode of operation whereas the 7 mA bias was chosen to keep both levels above threshold. When biased at 4 mA, the turn-on delay associated with subthreshold operation resulted in significant pattern dependent jitter as seen in Figure 10 at 6 Gb/s. The extent of the jitter indicates an upper limit of about 1 Gb/s in these operating conditions.

To further quantify the potential for these VCSELs to operate in this mode, the turn-on delay of both single mode and multimode lasers

Figure 9. Eye diagram generated by 12Gb/s digital modulation of a multimode VCSEL biased at 7 mA linked to a photodetector and inverting amplifier without filtering.

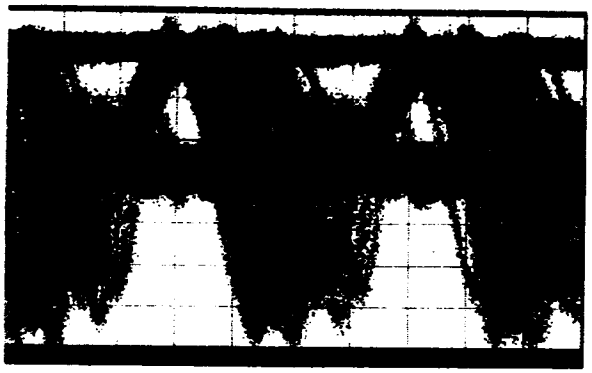

Figure 10. Eye diagram for the same configuration as in Figure 9 but biased at 4 mA and modulated at 6 Gb/s.

was measured for a variety of subthreshold biases. Pattern dependence was determined by using a repetitive pattern of 64 bits where only one bit was off. By varying the bit rate from 1 Gb/s to 12 Gb/s, the effect of off time on turn-on delay could be studied and used to infer the jitter associated with different lengths of off bit strings. The constant duty cycle approach reduces secondary effects due to varying heating or average bias level. Both the below threshold level and the high level were varied during the investigation.

Figure 11 shows the turn on delay as a function of the off time for the small single mode devices. Several curves are plotted for low levels of 0 V and 1 V and several different high levels ranging from 2.3 V (approximately 2 mA) to 3.8 V (approximately 4 mA). Note that these internal voltages are dropped across the 50 Ω source impedance in addition to the laser. The delay times for the two low levels are similar with the greatest difference occurring after short off times.

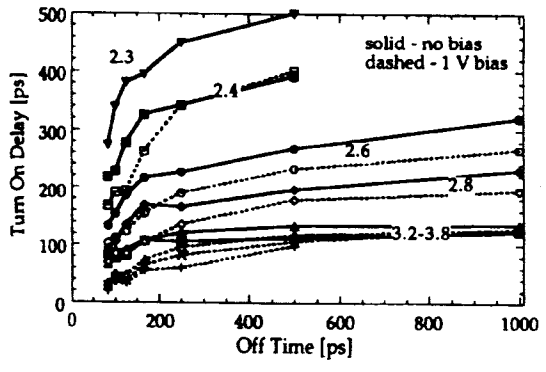

Figure 11. Turn on delay for a single mode VCSEL as a function of the preceding time off. The low (bias) and high levels are indicated for each curve.

When the high level is close to threshold, turn on maximum delay time can exceed 500 ps. Operation at several times threshold can make the delay as short as 120 ps. Still higher levels result in power saturation due to heating and give no shorter delay times.

The range of turn on delays for both the small and large lasers are summarized in Figure 11 to give an indication of pattern dependent jitter. The data is presented as a function of low level bias and grouped for a given high drive level. For long off times, the larger lasers are slightly slower at a given drive voltage. Increasing the low (bias) level doesn't substantially alter the turn on delay for long off times, but does shorten the delay after short off times. This is consistent with the subthreshold bias slowing carrier density decay from the active region but not providing enough steady state carrier concentrations to alter the turn on delay. The result is that subthreshold bias actually increases pattern dependent jitter but does not alter maximum turn on delay. Hence, 0 V bias is likely to be as attractive as higher levels of subthreshold bias.

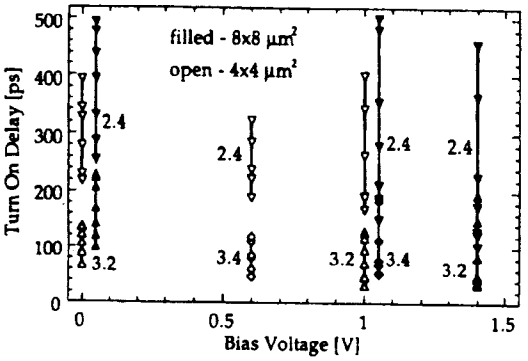

Figure 12. Ranges of turn on delay for varied off time and thus pattern dependent jitter are indicated for different bias and drive voltages.

Summary

While oxide confinement structures improve many parameters of VCSELs, it is also necessary to minimize the associated capacitance. Oxide confined VCSELs generate high photon densities by providing strong optical confinement and permitting operation to many times threshold through the combined benefits of low thresholds and high efficiency. The use of proton implantation has been described for reducing the oxide capacitance and increasing the electrical

bandwidth beyond other factors. This has produced bandwidths up to 21.5 GHz at which point the present VCSELs are believed to be thermally limited. Additional improvements should be obtained with improved heatsinking and higher efficiencies. Structures can also be designed to minimize the detrimental effects of ion implantation on resistance and thus optimize the resistance vs. capacitance tradeoff.

Large signal modulation at data rates up to 12 Gb/s have been demonstrated. Despite these advances, below threshold bias still results in substantial turn on delay and pattern dependent jitter. To quantify the latter, turn on delay vs. off time under a variety of bias conditions has been studied and reported. Smaller, single mode devices do have lower turn-on times compared to large, multimode devices driven to the same number of times threshold.

Acknowledgments

The authors would like to thank C. Tigges for help in computer modeling of microwave circuits and F. Cajas and J. Nevers for technical assistance with measurements. This work was performed at Sandia, a multiprogram laboratory operated by Lockheed Martin for the United States Department of Energy. under Contract DE-AC04-94AL85000. K. Lear is presently with MicroOptical Devices Inc., 5601C Midway Park Pl. NE, Albuquerque, NM 87109 where this manuscript was prepared. M. Ochiai is presently with Hewlett Packard's Optoelectronics Division in San Jose, CA. J. Banas is presently with the University of New Mexico, Center for High Technology Materials, Albuquerque, NM. J. Zolper is presently with the Office of Naval Research in Washington, DC. S. Kilcoyne is presently with Gore Photonics in Lompoc, CA.

References

[1] K. L. Lear, A. Mar, K. D. Choquette, S. P. Kilcoyne, R. P. Schneider, Jr., and K. M. Geib, "High-frequency modulation of oxide-confined vertical cavity surface emitting lasers", *Electron. Lett.* **32**(5), 457 (1996).

[2] K. D. Choquette, K. L. Lear, R. P. Schneider, Jr., K. M. Geib, J. J. Figiel, and R. Hull, "Fabrication and Performance of Selectively Oxidized Vertical-Cavity Lasers", *Photon. Tech. Lett.*, **7**(11), 1237 (1995).

[3] K. L. Lear, H. Q. Hou, J. J. Banas, B. E. Hammons, J. Furioli, and M. Osinski, "Vertical cavity laser on p-doped substrates", *Electron. Lett.* **33**(9), 783 (1997).

[4] B. J. Thibeault, K. Bertilsson, E. R. Hegblom, E. Strzelecka, P. D. Floyd, R. Naone, and L. A. Coldren, "High-Speed Characteristics of Low-Optical Loss Oxide-Apertured Vertical-Cavity Lasers", *Photon. Tech. Lett.*, **9**(1), 11 (1997).